

the real technical challenge. The diffraction rings in the star's diffraction pattern completely swamp the faint signal from the planet.

11.3 The Array Theorem

In this section we develop the array theorem, which is used for calculating the Fraunhofer diffraction from an array of N identical apertures. We will be using the theorem to compute diffraction from a grating, which may be thought of as a mask with many closely spaced identical slits. However, the array theorem can be applied to apertures with any shape and configuration, as suggested by Fig. 11.9.

Consider N apertures in a mask, each with the identical field distribution described by $E_{\text{aperture}}(x', y', 0)$. Each identical aperture has a unique location on the mask. Let the location of the n^{th} aperture be designated by the coordinates (x'_n, y'_n) . The field associated with the n^{th} aperture is then $E_{\text{aperture}}(x' - x'_n, y' - y'_n, 0)$, where the offset in the arguments shifts the location of the aperture. The field comprising all of the identical apertures is

$$E(x', y', 0) = \sum_{n=1}^N E_{\text{aperture}}(x' - x'_n, y' - y'_n, 0) \quad (11.19)$$

We next compute the Fraunhofer diffraction pattern for the above field. Upon inserting (11.19) into the Fraunhofer diffraction formula (10.19) we obtain

$$E(x, y, z) = -i \frac{e^{ikz} e^{i\frac{k}{2z}(x^2+y^2)}}{\lambda z} \sum_{n=1}^N \int_{-\infty}^{\infty} dx' \int_{-\infty}^{\infty} dy' E_{\text{aperture}}(x' - x'_n, y' - y'_n, 0) e^{-i\frac{k}{z}(xx' + yy')} \quad (11.20)$$

where we have taken the summation out in front of the integral. We have also integrated over the entire (infinitely wide) mask, taking E_{aperture} to be zero except inside each aperture.

Even without yet choosing the shape of the identical apertures, we can make some progress on (11.20) with the change of variables $x'' \equiv x' - x'_n$ and $y'' \equiv y' - y'_n$:

$$E(x, y, z) = -i \frac{e^{ikz} e^{i\frac{k}{2z}(x^2+y^2)}}{\lambda z} \sum_{n=1}^N \int_{-\infty}^{\infty} dx'' \int_{-\infty}^{\infty} dy'' E_{\text{aperture}}(x'', y'', 0) \times e^{-i\frac{k}{z}[x(x''+x'_n)+y(y''+y'_n)]} \quad (11.21)$$

Next we pull the factor $\exp\{-i\frac{k}{z}(xx'_n + yy'_n)\}$ out in front of the integral to arrive

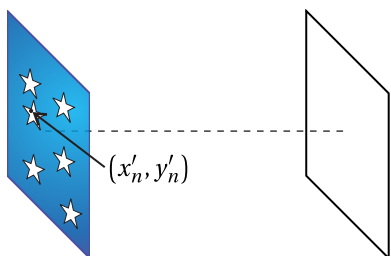


Figure 11.9 Array of identical apertures.

at our final result:

$$E(x, y, z) = \left[\sum_{n=1}^N e^{-i\frac{k}{z}(xx'_n + yy'_n)} \right] \times \left[-i \frac{e^{ikz} e^{i\frac{k}{2z}(x^2 + y^2)}}{\lambda z} \int_{-\infty}^{\infty} dx' \int_{-\infty}^{\infty} dy' E_{\text{aperture}}(x', y', 0) e^{-i\frac{k}{z}(xx' + yy')} \right] \quad (11.22)$$

For the sake of elegance, we have traded back x' for x'' and y' for y'' as the variables of integration. Equation (11.22) is known as the array theorem.³ Note that the second factor in brackets is exactly the Fraunhofer diffraction pattern from a single aperture centered on $x' = 0$ and $y' = 0$. When more than one identical aperture is present, we only need to evaluate the Fraunhofer diffraction formula for a single aperture. Then, the single-aperture result is multiplied by the summation in front, which contains entirely the information about the placement of the (many) identical apertures.

Example 11.2

Calculate the Fraunhofer diffraction pattern for two identical circular apertures with diameter D whose centers are separated by a spacing h .

Solution: As computed previously, the single-slit Fraunhofer diffraction pattern from a circular aperture is given by (10.29). This is multiplied by (the square of) the factor on the first line of the array theorem (11.22), which gives an overall intensity pattern of

$$I(x, y, z) = \left[\sum_{n=1}^2 e^{-i\frac{k}{z}(xx'_n + yy'_n)} \right]^2 \times I_0 \left(\frac{\pi D^2}{4\lambda z} \right)^2 \left[2 \frac{J_1(kD\rho/2z)}{(kD\rho/2z)} \right]^2$$

Let $y'_1 = y'_2 = 0$. To create the separation h , let $x'_1 = -h/2$ and $x'_2 = h/2$. Then

$$\sum_{n=1}^2 e^{-i\frac{k}{z}(xx'_n + yy'_n)} = e^{-i\frac{k}{z}\left(-\frac{hx}{2}\right)} + e^{-i\frac{k}{z}\left(\frac{hx}{2}\right)} = 2 \cos\left(\frac{khx}{2z}\right)$$

³A somewhat abstract alternative route to the array theorem recognizes that the field for each aperture can be written as a 2-D convolution (see P0.26) between the aperture function $E_{\text{aperture}}(x', y', 0)$ and delta functions specifying the aperture location:

$$E_{\text{aperture}}(x' - x'_n, y' - y'_n, 0) = \int_{-\infty}^{\infty} dx'' \int_{-\infty}^{\infty} dy'' \delta(x'' - x'_n) \delta(y'' - y'_n) E_{\text{aperture}}(x' - x'', y' - y'', 0)$$

The integral in (11.20) therefore may be viewed as a 2-D Fourier transform of a convolution, where kx/z and ky/z play the role of *spatial frequencies*. The convolution theorem (see P0.26) indicates that this is the same as the product of Fourier transforms. The 2-D Fourier transform for the delta function (times 2π) is

$$\int_{-\infty}^{\infty} dx'' \int_{-\infty}^{\infty} dy'' \delta(x'' - x'_n) \delta(y'' - y'_n) e^{-i\frac{k}{z}(xx'' + yy'')} = e^{-i\frac{k}{z}(xx'_n + yy'_n)}$$

The array theorem (11.22) exhibits this factor. It multiplies the single-slit Fraunhofer diffraction integral, which is the Fourier transform of the other function.

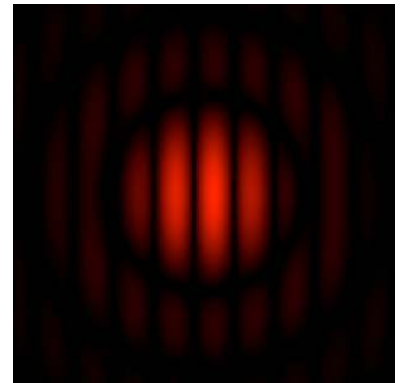


Figure 11.10 Fraunhofer diffraction pattern from two identical circular holes separated by twice their diameters.

The overall pattern then becomes

$$I(x, y, z) = I_0 \left(\frac{\pi \ell^2}{2\lambda z} \right)^2 \left[2 \frac{J_1(kD\rho/2z)}{(kD\rho/2z)} \right]^2 \cos^2 \left(\frac{khx}{2z} \right)$$

This pattern can be seen in Fig. 11.10.

11.4 Diffraction Grating

In this section we will use the array theorem to calculate the Fraunhofer diffraction from a grating comprised of an array of equally spaced identical slits. An array of uniformly spaced slits is called a transmission grating (see Fig. 11.11). Reflection gratings are similar, being composed of an array of narrow rectangular mirrors that behave similarly to the slits.

Let the slit apertures be positioned at

$$x'_n = \left(n - \frac{N+1}{2} \right) h, \quad y'_n = 0 \quad (11.23)$$

where N is the total number of slits. Then the summation in the array theorem, (11.22), becomes

$$\sum_{n=1}^N e^{-i \frac{k}{z} (xx'_n + yy'_n)} = e^{i \frac{khx}{z} \left(\frac{N+1}{2} \right)} \sum_{n=1}^N e^{-i \frac{khx}{z} n} \quad (11.24)$$

This summation is recognized as a geometric sum, which can be performed using formula (0.65). Equation (11.24) then simplifies to

$$\begin{aligned} \sum_{n=1}^N e^{-i \frac{k}{z} (xx'_n + yy'_n)} &= e^{i \frac{k}{z} \left(\frac{N+1}{2} \right) xh} e^{-i \frac{khx}{z}} \frac{e^{-i \frac{khx}{z} N} - 1}{e^{-i \frac{khx}{z}} - 1} \\ &= \frac{e^{-i \frac{khx}{2z} N} - e^{i \frac{khx}{2z} N}}{e^{-i \frac{khx}{2z}} - e^{i \frac{khx}{2z}}} = \frac{\sin \left(N \frac{khx}{2z} \right)}{\sin \left(\frac{khx}{2z} \right)} \end{aligned} \quad (11.25)$$

The diffraction pattern for a single slit was previously calculated in example 10.4. When (11.25) and (10.20) are installed in the array theorem (11.22), we get for the intensity

$$I(x, y, z) = \frac{\sin^2 \left(N \frac{khx}{2z} \right)}{\sin^2 \left(\frac{khx}{2z} \right)} \left[I_0 \frac{\Delta x^2 \Delta y^2}{\lambda^2 z^2} \operatorname{sinc}^2 \left(\frac{\pi \Delta x}{\lambda z} x \right) \operatorname{sinc}^2 \left(\frac{\pi \Delta y}{\lambda z} y \right) \right] \quad (11.26)$$

This is the Fraunhofer diffraction pattern for the overall grating.

The y dependence in (11.26) is typically unimportant in applications where spectral information is revealed in the x -dimension only. Moreover, the incident field often does not have a uniform strength along the entire slit in the

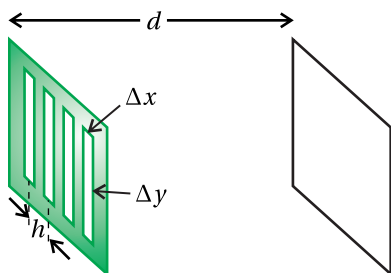


Figure 11.11 Transmission grating.

y -dimension, making the diffraction pattern along the y dimension different from $\text{sinc}[(\pi\Delta y/\lambda z)y]$ anyway. Since y is of little relevance, we can consider the pattern in (11.26) for fixed y , say $y = 0$. The intensity pattern in the horizontal dimension may be written as

$$I(x) = I_{\text{peak}} \text{sinc}^2\left(\frac{\pi\Delta x}{\lambda z}x\right) \frac{\sin^2\left(N\frac{\pi hx}{\lambda z}\right)}{N^2 \sin^2\left(\frac{\pi hx}{\lambda z}\right)} \quad (11.27)$$

Note that $\lim_{\alpha \rightarrow 0} \frac{\sin N\alpha}{\sin \alpha} = N$ so we have placed N^2 in the denominator and absorbed the same factor into the definition of I_{peak} , which represents the intensity on the screen at $x = 0$. Again, the intensity I_{peak} is associated with a given value of y .

It is left as an exercise to study the functional form of (11.27), especially how the number of slits N influences the behavior. The case of $N = 2$ describes the diffraction pattern for a Young's double slit experiment. We now have a description of the Young's two-slit pattern in the case that the slits have finite openings of width Δx rather than infinitely narrow ones.

11.5 Spectrometers

The formula (11.27) can be exploited to make wavelength measurements. This forms the basis of a diffraction grating spectrometer. In order to achieve good spatial separation between wavelengths, it is necessary to allow the light to propagate a far distance. Optimal wavelength separation therefore occurs in the Fraunhofer regime for which (11.27) applies.

A spectrometer has relatively poor resolving power compared to a Fabry-Perot interferometer. Nevertheless, a spectrometer is not hampered by the serious limitation imposed by free spectral range. A spectrometer is able to measure a wide range of wavelengths simultaneously. The Fabry-Perot interferometer and the grating spectrometer in this sense are complementary, the one being able to make very precise measurements within a narrow wavelength range and the other being able to characterize wide ranges of wavelengths simultaneously.

To appreciate how a spectrometer works, consider Fraunhofer diffraction from a grating, as described by (11.27). The structure of the diffraction pattern has various peaks. For example, Fig. 11.12a shows the diffraction peaks from a Young's double slit (i.e. $N = 2$). The diffraction pattern is comprised of the typical Young's double-slit pattern multiplied by the diffraction pattern of a single slit. (Note that $\sin^2\left(2\frac{\pi hx}{\lambda z}\right)/4\sin^2\left(\frac{\pi hx}{\lambda z}\right) = \cos^2\left(\frac{\pi hx}{\lambda z}\right)$.)

As the number of slits N increases, the peaks tend to sharpen while staying in the same location as the peaks in the Young's double-slit pattern. Figure 11.12b shows the case for $N = 5$. The prominent peaks occur when $\sin(\pi hx/\lambda z)$ in the denominator of (11.27) goes to zero. Keep in mind that the numerator goes to zero at the same places, creating a zero-over-zero situation, so the peaks are not infinitely tall.

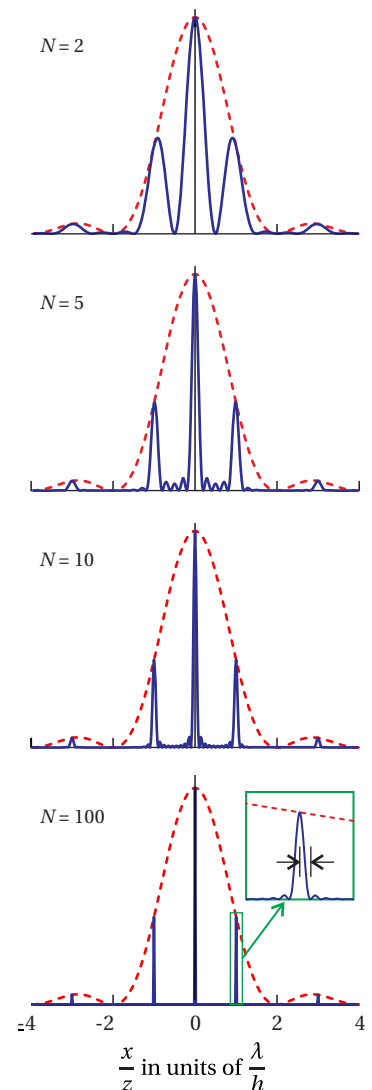


Figure 11.12 Diffraction through various numbers of slits, each with $\Delta x = h/2$ (slit widths half the separation). The dotted line shows the single slit diffraction pattern. (a) Diffraction from a double slit. (b) Diffraction from 5 slits. (c) Diffraction from 10 slits. (d) Diffraction from 100 slits.

With larger values of N , the peaks can become extremely sharp, and the small secondary peaks in between become tiny in comparison. Fig. 11.12c shows the case of $N = 10$ and Fig. 11.12d, shows the case of $N = 100$.

When very many slits are used, the resulting sharp diffraction peaks becomes very useful for measuring spectra of light, since the position of the diffraction peaks depends on wavelength (except for the center peak at $x = 0$). If light of different wavelengths is simultaneously present, then the diffraction peaks associated with different wavelengths appear in different locations.

Consider the inset in Fig. 11.12d, which gives a close-up view of the first-order diffraction peak for $N = 100$. The location of this peak on a distant screen varies with the wavelength of the light. How much must the wavelength change to cause the peak to move by half of its 'width' as marked in the inset of Fig. 11.12d? This corresponds to the minimum wavelength separation that allows two associated peaks to be distinguished.

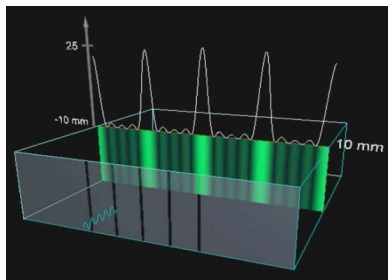


Figure 11.13 Animation showing diffraction through a number of slits.

Finding the Minimum Distinguishable Wavelength Separation

As mentioned, the main diffraction peaks occur when the denominator of (11.27) goes to zero, i.e.

$$\frac{\pi h x}{\lambda z} = m\pi \quad (11.28)$$

The numerator of (11.27) goes to zero at these same locations (i.e. $N\pi h x/\lambda z = Nm\pi$), so the peaks remain finite. If two nearby wavelengths λ_1 and λ_2 are sent through the grating simultaneously, their m^{th} peaks are located at

$$x_1 = \frac{mz\lambda_1}{h} \quad \text{and} \quad x_2 = \frac{mz\lambda_2}{h} \quad (11.29)$$

These are spatially separated by

$$\Delta x_\lambda \equiv x_2 - x_1 = \frac{mz}{h} \Delta\lambda \quad (11.30)$$

where $\Delta\lambda \equiv \lambda_2 - \lambda_1$.

Meanwhile, we can find the spatial width of, say, the first peak by considering the change in x_1 that causes the sine in the numerator of (11.27) to reach the nearby zero (see inset in Fig. 11.12d). This condition implies

$$N \frac{\pi h (x_1 + \Delta x_{\text{peak}})}{\lambda_1 z} = Nm\pi + \pi \quad (11.31)$$

We will say that two peaks, associated with λ_1 and λ_2 , are barely distinguishable when $\Delta x_\lambda = \Delta x_{\text{peak}}$. We also substitute from (11.29) to rewrite (11.31) as

$$N \frac{\pi h (mz\lambda_1/h + mz\Delta\lambda/h)}{\lambda_1 z} = Nm\pi + \pi \quad \Rightarrow \quad \Delta\lambda = \frac{\lambda}{Nm} \quad (11.32)$$

Here we have dropped the subscript on the wavelength in the spirit of $\lambda_1 \approx \lambda_2 \approx \lambda$.

As we did for the Fabry-Perot interferometer, we can define the *resolving power* of the diffraction grating as

$$RP \equiv \frac{\lambda}{\Delta\lambda} = mN \quad (11.33)$$

The resolving power is proportional to the number of slits illuminated on the diffraction grating. The resolving power also improves for higher diffraction orders m .

Example 11.3

What is the resolving power with $m = 1$ of a 2-cm-wide grating with 500 slits per millimeter, and how wide is the 1st-order diffraction peak for 500-nm light after 1-m focusing?

Solution: From (11.33) the resolving power is

$$RP = mN = 2 \text{ cm} \frac{500}{0.1 \text{ cm}} = 10^4$$

and the minimum distinguishable wavelength separation is

$$\Delta\lambda = \lambda/RP = 500 \text{ nm}/10^4 = 0.05 \text{ nm}$$

From (11.30), with $z \rightarrow f$, we have

$$\Delta x = \frac{mf}{h} \Delta\lambda = \frac{1 \text{ m}}{2 \times 10^{-6} \text{ m}} 0.05 \text{ nm} = 25 \mu\text{m}$$

As illustrated in the previous example, it is common to employ a focusing optic to reach the Fraunhofer limit within a convenient distance. In addition, since the array theorem requires the same illumination of each slit, the incident light should be collimated or plane-wave like. This is also accomplished using a lens. Fig. 11.14 illustrates the typical layout. Light enters a narrow slit located at the focus of a concave mirror. The collimated light then strikes a reflective diffraction grating. The first-order diffracted light is then focused by a second concave mirror where the Fraunhofer diffraction of the grating appears. If a CCD camera is positioned at the focus to record many wavelengths at once, the instrument is called a spectrometer. If instead an exit slit is placed at the focus so that only one wavelength at a time emerges through the slit, the instrument is called a monochromator. In the latter case, the angle of the grating can be scanned to cause different wavelengths to transmit through the exit slit.

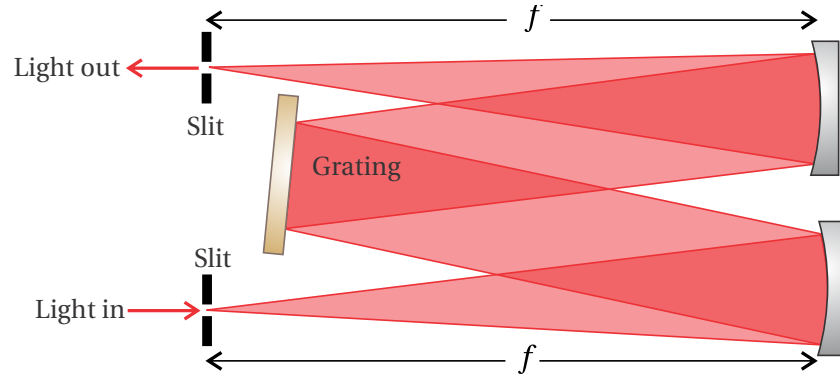


Figure 11.14 Symmetric monochromator layout.

11.6 Diffraction of a Gaussian Field Profile

Consider a Gaussian field profile (in the plane $z = 0$) described with the functional form

$$E(x', y', 0) = E_0 e^{-\frac{x'^2 + y'^2}{w_0^2}} \quad (11.34)$$

The parameter w_0 is called the *beam waist*, which specifies the radius of Gaussian profile. It is depicted in Fig. 11.15. To better appreciate the meaning of w_0 , consider the intensity of the above field distribution:

$$I(x', y', 0) = I_0 e^{-2\rho^2/w_0^2} \quad (11.35)$$

where $\rho'^2 \equiv x'^2 + y'^2$. In (11.35) we see that w_0 indicates the radius at which the intensity reduces by the factor $e^{-2} = 0.135$.

We would like to know how this field evolves when it propagates forward from the plane $z = 0$. Notice that the phase of (11.34) is uniform or plane-wave like. We therefore expect the beam to expand outward as it diffracts along z .⁴ We compute the field downstream using the Fresnel approximation (10.13):

$$E(x, y, z) = -i \frac{e^{ikz} e^{i\frac{k}{2z}(x^2 + y^2)}}{\lambda z} \int_{-\infty}^{\infty} dx' \int_{-\infty}^{\infty} dy' \left[E_0 e^{-(x'^2 + y'^2)/w_0^2} \right] e^{i\frac{k}{2z}(x'^2 + y'^2)} e^{-i\frac{k}{z}(xx' + yy')} \quad (11.36)$$

The Gaussian profile itself limits the dimension of the ‘aperture’, so there is no problem with integrating to infinity. Equation (11.36) can be rewritten as

$$E(x, y, z) = -i \frac{E_0 e^{ikz} e^{i\frac{k}{2z}(x^2 + y^2)}}{\lambda z} \int_{-\infty}^{\infty} dx' e^{-\left(\frac{1}{w_0^2} - i\frac{k}{2z}\right)x'^2 - i\frac{kx}{z}x'} \int_{-\infty}^{\infty} dy' e^{-\left(\frac{1}{w_0^2} + i\frac{k}{2z}\right)y'^2 - i\frac{ky}{z}y'} \quad (11.37)$$

⁴The beam would converge to narrower widths if instead we used a phase associated with converging wavefronts like those on the left of Fig. 11.17.

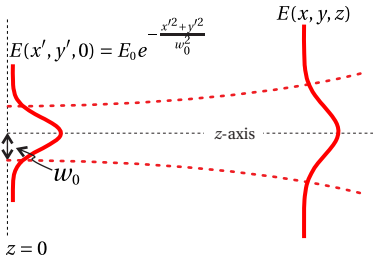


Figure 11.15 Diffraction of a Gaussian field profile.